doi: 10.18323/2782-4039-2025-3-73-9

The influence of rotary swaging and subsequent annealing on the structure and mechanical properties of L68 single-phase brass

Eleonora I. Chistyukhina*[1,2,4], research engineer
at the Laboratory of Physical Metallurgy of Non-Ferrous and Light Metals named by Academician A.A. Bochvar, graduate student of Chair of Metal Science and Physics of Strength
Natalia S. Martynenko[1,5], PhD (Engineering), senior researcher
at the Laboratory of Physical Metallurgy of Non-Ferrous and Light Metals named by Academician A.A. Bochvar
Olga V. Rybalchenko[1,6], PhD (Engineering), leading researcher
at the Laboratory of Physical Metallurgy of Non-Ferrous and Light Metals named by Academician A.A. Bochvar
Ivan S. Nikitin[3,7], PhD (Engineering), junior researcher
at the Laboratory of Mechanical Properties of Nanostructured Materials and Superalloys
Elena A. Lukyanova[1,8], PhD (Engineering), senior researcher
at the Laboratory of Physical Metallurgy of Non-Ferrous and Light Metals named by Academician A.A. Bochvar
Artem D. Gorbenko[1,9], research engineer
at the Laboratory of Strength and Plasticity of Metallic and Composite Materials and Nanomaterials
Diana R. Temralieva[1,10], research engineer
at the Laboratory of Physical Metallurgy of Non-Ferrous and Light Metals named by Academician A.A. Bochvar
Petr B. Straumal[1,11], PhD (Physics and Mathematics), senior researcher
at the Laboratory of Physical Metallurgy of Non-Ferrous and Light Metals named by Academician A.A. Bochvar
Vladimir A. Andreev[1,12], PhD (Engineering), leading researcher
at the Laboratory of Plastic Deformation of Metallic Materials
Sergey V. Dobatkin[1,13], Doctor of Science (Engineering), Professor, Head
of the Laboratory of Physical Metallurgy of Non-Ferrous and Light Metals named by Academician A.A. Bochvar

[1]*A.A. Baikov Institute of Metallurgy and Materials Science of RAS, Moscow (Russia)*
[2]*University of Science and Technology "MISIS", Moscow (Russia)*
[3]*Belgorod State University, Belgorod (Russia)*

***E-mail:** e.chistyuhina@mail.ru

[4]ORCID: https://orcid.org/0009-0009-2192-3246
[5]ORCID: https://orcid.org/0000-0003-1662-1904
[6]ORCID: https://orcid.org/0000-0002-0403-0800
[7]ORCID: https://orcid.org/0000-0002-5417-9857
[8]ORCID: https://orcid.org/0000-0001-7122-6427
[9]ORCID: https://orcid.org/0000-0002-3357-4049
[10]ORCID: https://orcid.org/0000-0002-8392-7826
[11]ORCID: https://orcid.org/0000-0001-6192-5304
[12]ORCID: https://orcid.org/0000-0003-3937-1952
[13]ORCID: https://orcid.org/0000-0003-4232-927X

Received 30.06.2025 *Revised 18.07.2025* *Accepted 25.08.2025*

Abstract: Copper alloys based on the Cu–Zn system, in particular L68 brass, are promising structural materials. However, to improve their reliability and expand the scope of application, it is necessary to enhance their strength characteristics. In this work, the influence of a combination of rotary swaging (RS) and subsequent annealing on the structure, strength and ductility of L68 brass was studied. For this purpose, the alloy microstructure was studied in the quenched and deformed states, mechanical tests for uniaxial tension, a Brinell hardness study, and an assessment of structural and phase transitions using differential scanning calorimetry were carried out. It was found that during rotary swaging, both α-phase grains elongated along the deformation direction and an ultrafine-grained structure inside them consisting of subgrains, deformation twins and shear bands are formed. Subsequent annealing at 450 °C leads to an increase in the grain size to 3–5 μm due to static recrystallization. After rotary swaging, an increase in the offset yield strength ($\sigma_{0.2}$) and ultimate tensile stress limit (σ_B) by ~10 and ~3.5 times, respectively, is observed with a decrease in the relative elongation value by more than 6 times. Subsequent annealing at 450 °C, which caused the formation of a recrystallised structure, led to a decrease in the strength characteristics of L68 brass relative to the deformed state with a simultaneous increase in the relative elongation value compared to both the deformed and the initial state of the alloy. However, it is worth noting that $\sigma_{0.2}$ and σ_B of L68 brass after rotary swaging

and subsequent annealing at 450 °C exceed the values for the quenched alloy by an average of ~2.5 and ~1.7 times, respectively, and exceed the values regulated by GOST 494-90, GOST 1066-2015, GOST 931-90, and GOST 5362-78.

Keywords: L68 brass; rotary swaging; ultrafine-grained structure; recrystallization; strength; ductility.

Acknowledgments: The work was carried out with the financial support of state assignment No. 075-00319-25-00.

The paper was written on the reports of the participants of the XII International School of Physical Materials Science (SPM-2025), Togliatti, September 15–19, 2025.

For citation: Chistyukhina E.I., Martynenko N.S., Rybalchenko O.V., Nikitin I.S., Lukyanova E.A., Gorbenko A.D., Temralieva D.R., Straumal P.B., Andreev V.A., Dobatkin S.V. The influence of rotary swaging and subsequent annealing on the structure and mechanical properties of L68 single-phase brass. *Frontier Materials & Technologies*, 2025, no. 3, pp. 113–124. DOI: 10.18323/2782-4039-2025-3-73-9.

INTRODUCTION

Copper and its alloys are widely used in the electrical industry due to their excellent electrical conductivity [1]. However, copper alloys, in particular alloys of the Cu–Zn system, are also used as structural materials in shipbuilding and aircraft construction, the petrochemical industry, in the production of pipes and plumbing products, as well as refrigeration equipment and military products [2]. This use of brasses is caused by their high corrosion resistance, non-magnetic nature and good formability, as well as by a balance of strength and ductility [3]. Brass with a zinc content of up to 37 % is single-phase and is an α-solid solution with a face-centered cubic lattice [4]. Single-phase α-brass with a low zinc content is more resistant to corrosion and dezincification processes compared to two-phase (α+β)-brasses [5; 6]. However, the main disadvantage of single-phase brasses is their low strength characteristics. Precipitation hardening and grain refinement by deformation treatment can improve the mechanical properties and, consequently, expand the scope of application of brass. In this case, by refining the microstructure to an ultrafine-grained (UFG) and/or nanosized structure, it is possible to achieve a significant increase in the strength of copper alloys. Nano- and UFG structures in metals and alloys can be formed by the severe plastic deformation (SPD) methods [7]. The most popular SPD methods applied to copper alloys are high-pressure torsion [8], equal-channel angular pressing (ECAP) [9], multi-axial forging [10], etc. Thus, in [11], the authors managed to achieve a combination of relatively high strength and ductility in the Cu–30Zn alloy treated with ECAP. In this case, the ultimate tensile stress limit of the alloy was 565 MPa, the yield strength was 250 MPa, and the relative elongation was 20 %. In another work, after ECAP, it was possible to achieve significant strengthening of the Cu–30Zn alloy ($\sigma_{0.2}$=542 MPa, σ_B=692 MPa) accompanied by a strong drop in ductility (up to δ=5.6 %) [11]. However, despite the advantages of SPD methods for strengthening metals and alloys, their application in industry is still hindered. Therefore, the development of processing modes that allow obtaining a UFG structure in copper alloys without using SPD methods is an urgent task.

In copper alloys, it is possible to obtain a UFG structure by using traditional deformation methods. For example, in work [12], a UFG structure was obtained in Cu–30Zn brass using cryogenic rolling followed by recrystallization annealing. In this case, a decrease in the average grain size to 0.5 μm with a proportion of high-angle boundaries equal to 90 % made it possible to double the strength of the original alloy. Another traditional deformation method successfully used to improve the physical and mechanical properties of materials by creating a UFG structure is rotary swaging (RS). Traditionally, this method is used to manufacture hollow and solid, cylindrical and stepped shafts and axles with a round and faceted cross-section, therefore, its manufacturing application is not difficult, unlike SPD methods [13]. Currently, rotary swaging is successfully used to refine the structure of structural titanium [14; 15] and aluminium [16] alloys, steels [17] and other materials. Previously, we have already demonstrated the potential of rotary swaging for producing a UFG structure in copper alloys: thus, studies were conducted on the influence of rotary swaging on the microstructure, mechanical properties and electrical conductivity of Cu–0.8%Hf [18], Cu–0.77%Cr–0.86%Hf [19] and Cu–0.5%Cr–0.08%Zr [20; 21] alloys. In these alloys, due to the formed UFG structure, as well as the deposition of particles rich in Cr, Zr and Hf, the strength and electrical conductivity increase significantly with a simultaneous decrease in ductility.

The aim of the work is to study the influence of rotary swaging and subsequent annealing on the structure and mechanical properties of single-phase L68 brass. It is expected that the combination of rotary swaging and subsequent annealing will allow producing an alloy with improved strength and ductility.

METHODS

The material of the study was L68 grade brass. For smelting the studied alloy, M0b grade copper and Ts0 grade zinc were used as charge materials. The alloy was smelted in an induction furnace; casting was carried out in a water-cooled cast-iron mold with a diameter of 52 mm and a height of 200 mm. The chemical composition was determined using X-ray fluorescence analysis on a BRUKER S8 Tiger (series 2, Germany) sequential X-ray fluorescence wave-dispersive spectrometer in a vacuum according to the standard technique using the QUANT-EXPRESS software (Bruker, Germany). According to the analysis, the studied alloy consisted of 68±0.21 wt. % of Cu and 32±0.13 wt. % of Zn. Then, the resulting ingot was subjected to hot pressing at a temperature of 630 °C to a final diameter of 20 mm. Then, the rod was annealed at 800 °C for 2 h, followed by quenching in water.

Rotary swaging was performed at room temperature using an RKM 2129.02 two-die rotary swaging machine. Before rotary swaging, the rod was mechanically turned to 19 mm (initial diameter). Rotary swaging was performed in 10 passes with an intermediate reduction in the rod diame-

ter from 0.6 to 1.5 mm, depending on the stage of deformation to a final diameter of 6 mm.

The degree of deformation (ε) was determined by the formula

$$\varepsilon = \ln \frac{A_0}{A_f},$$

where A_0 is the initial cross-sectional area of the blank;
A_f is the final cross-sectional area of the blank.

Therefore, the degree of deformation corresponding to the final diameter of the rod of 6 mm was equal to 2.31.

The microstructure before and after rotary swaging was studied at low magnifications using an ADF I350 optical microscope (ADF OPTICS Co. LTD, China). The microstructure after rotary swaging was analysed in the longitudinal section of the rod, parallel to the deformation direction. The microstructure after rotary swaging was studied using transmission electron microscopy (TEM). TEM analysis was performed using a JEOL JEM 2100 microscope (Japan) at an accelerating voltage of 200 kV. Samples for transmission microscopy were prepared by electrolytic polishing on a TenuPol 5 installation (Denmark) using an electrolyte containing HNO_3 and CH_3OH at a voltage of 19.5 V and a temperature of −25 °C. The size of the structural components was determined by the random linear intercept method in the Digimizer software environment.

The structural phase transitions were studied by differential scanning calorimetry (DSC) on a NETZSCH DSC 404 F3 Pegasus device (NETZSCH, Germany) with linear heating in the temperature range of 150–700 °C in a protective argon atmosphere at a rate of 10 K/min in corundum crucibles. To understand better the reactions occurring during heating of the studied samples, overlapping peaks were separated. The obtained experimental data were described as a superposition of Gaussian peaks, or Gaussians, meaning the addition of several Gaussian functions. Origin Pro 2021 software was used to perform peak separation analysis. The resulting function was obtained, which had several maxima describing the transformations occurring during heating.

For uniaxial tensile tests, flat samples with a working part length of 5.75 mm, a width of 2 mm and a thickness of 1 mm were prepared. Mechanical tests were carried out at room temperature on an Instron 3382 testing machine (UK) at a constant loading rate of 1 mm/min. At least three samples were tested for each alloy state. Hardness was measured by the Brinell method on an IT 5010-01 testing machine (Russia) with a steel indenter diameter of 2.5 mm under a load of 62.5 kg, holding time of 30 s.

RESULTS

Fig. 1 shows that the structure of L68 brass in the quenched state consists of large α-phase grains 500–600 μm in size and annealing twins 10 to 70 μm in size. The microstructure is significantly transformed during rotary swaging. After rotary swaging, bands about 45 μm wide elongated along the swaging direction are formed.

After rotary swaging, a UFG structure is formed inside the elongated α-phase grains (Fig. 2 a). This UFG structure consists of deformation twins from several tens to 200 nm in width (Fig. 2 b), subgrains 300–400 nm in size, the boundaries of which are lined up with wide dislocation walls (Fig. 2 c), and shear bands 400–500 nm in width (Fig. 2 a). It should also be noted that the formation of subgrains occurs mostly inside the shear bands (Fig. 2 a).

Fig. 3 combines the original experimental data, the individual obtained approximation peaks for the studied alloys, and a new resulting line (cumulative curve) of the approximation of overlapping peaks based on the estimated values. One can see that the new fitted profile is almost identical to the experimental one (Fig. 3), which reflects the accuracy of the peak separation procedure used in this analysis.

The DSC analysis of the alloy curve revealed the presence of five heat absorption peaks: two small peaks corresponding to temperatures of ~213 and ~301 °C, the maximum peak at ~433 °C, and peaks at ~560 and ~626 °C

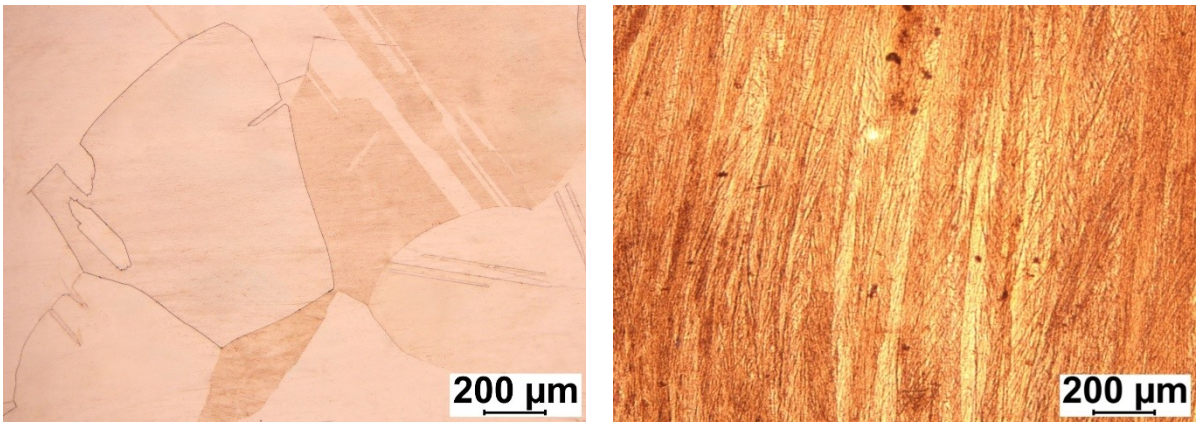

a *b*

Fig. 1. *Microstructure of L68 brass in the quenched state (**a**) and after rotary swaging at room temperature (**b**)*
Рис. 1. *Микроструктура латуни Л68 в закаленном состоянии (**а**) и после ротационной ковки при комнатной температуре (**b**)*

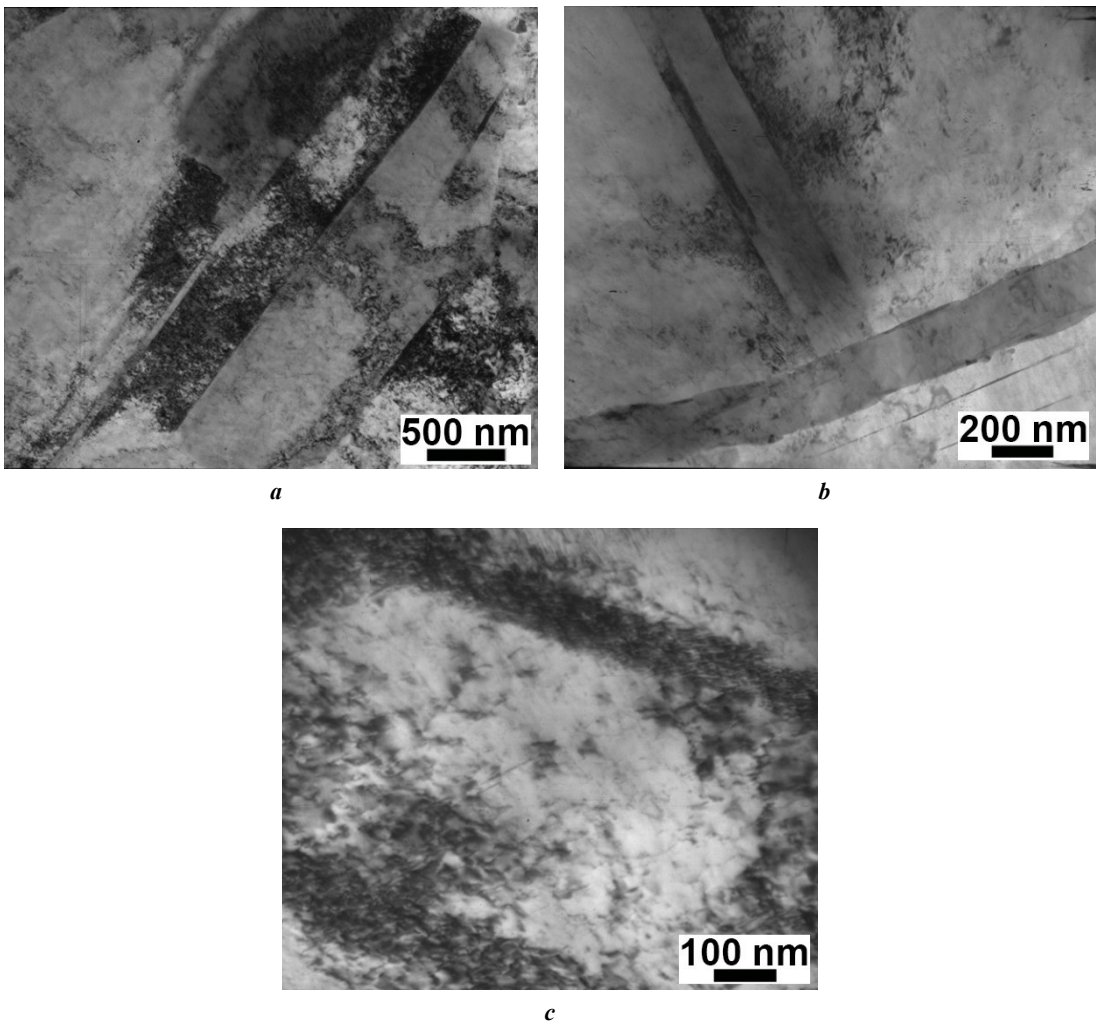

a *b*

c

Fig. 2. *TEM images of L68 brass after rotary swaging: alloy structure at magnifications of ×25,000 (**a**), ×50,000 (**b**) and ×100,000 (**c**)*
Рис. 2. *ПЭМ-изображения латуни Л68 после ротационной ковки: структура сплава при увеличениях ×25 000 (**a**), ×50 000 (**b**) и ×100 000 (**c**)*

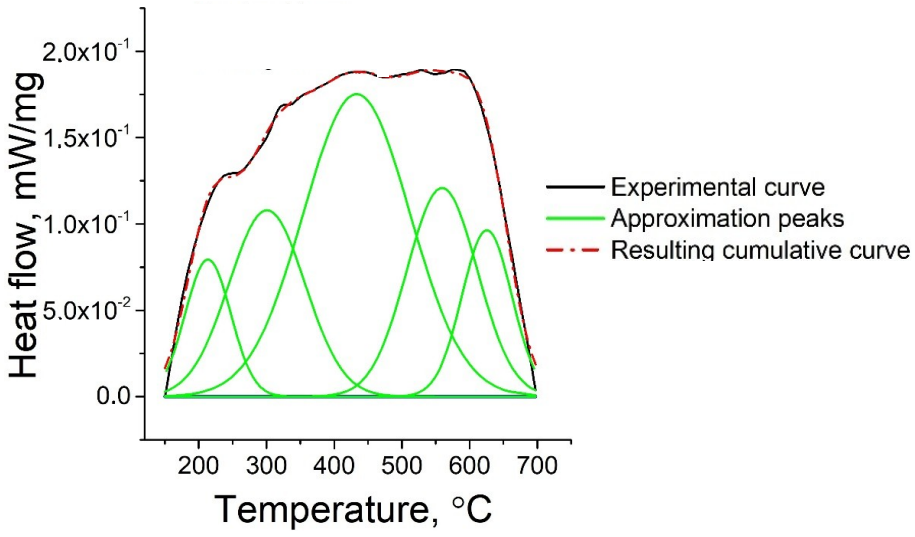

Fig. 3. *Dependence of heat flow on heating temperature for L68 brass after rotary swaging*
Рис. 3. *Зависимость теплового потока от температуры нагрева для латуни Л68 после ротационной ковки*

(Fig. 3). Based on the obtained results, the temperature regimes of 450, 500, and 550 °C were determined for subsequent annealing of L68 brass after rotary swaging. The choice of temperatures was based on the fact that structural and phase transformations should already occur at these temperatures. In this case, temperatures above 550 °C were not taken into account to avoid rapid grain growth.

It can be seen from Fig. 4 that additional annealing of the alloy after rotary swaging leads to a decrease in hardness, the higher the heating temperature. At the same time, in the range of 30–240 min, the holding time does not have a significant effect on the hardness values.

After quenching, the alloy demonstrates high ductility values with relatively low strength properties (Fig. 5). Carrying out rotary swaging with a degree of deformation of 2.31 significantly increases the values of strength characteristics, while the elongation decreases. After additional annealing, the strength characteristics decrease compared to the values after rotary swaging, but relative to the quenched state, the ultimate tensile stress limit, offset yield strength and elongation increase.

Table 1 shows that rotary swaging at ε=2.31 resulted in a significant increase in strength with an increase in the values of $\sigma_{0.2}$ and σ_B by more than 10 and 3 times, respectively, while δ decreased by more than 6 times.

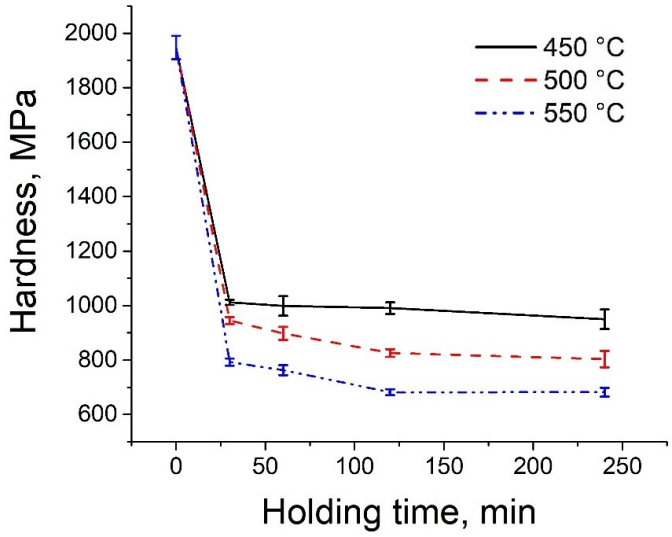

Fig. 4. *Dependence of the hardness of L68 brass after rotary swaging on the temperature and heating time*
Рис. 4. *Зависимость твердости латуни Л68 после ротационной ковки от температуры и времени нагрева*

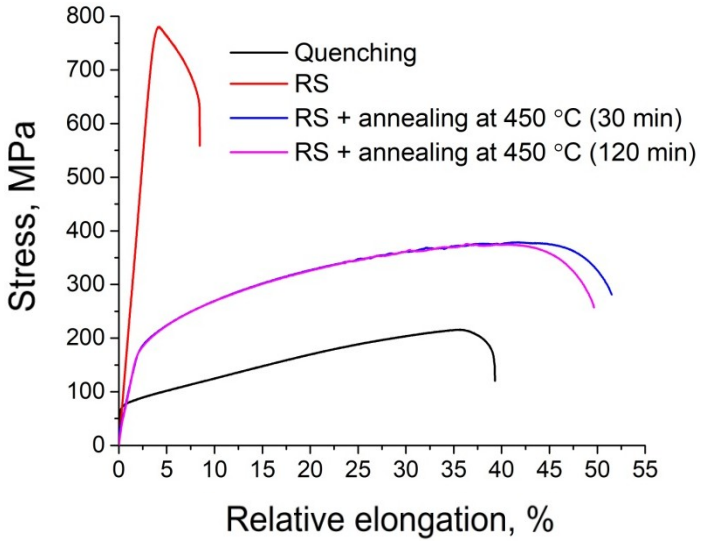

Fig. 5. *Stress-strain curves of L68 brass in different states*
Рис. 5. *Кривые растяжения латуни Л68 в различных состояниях*

Table 1. *Mechanical properties of L68 brass in different states*
Таблица 1. *Механические свойства латуни Л68 в различных состояниях*

State		$\sigma_{0.2}$, MPa	σ_B, MPa	δ, %
Quenching		72±4	222±13	39.9±3.8
Rotary swaging at ε=2.31	before heating	754±5	775±6	6.3±0.4
	450 °C (30 min)	180±2	382±4	49.1±1.4
	450 °C (2 h)	172±3	374±4	49.9±2.8

Additional annealing at 450 °C for 30 and 120 min after rotary swaging contributed to a decrease in strength properties and an increase in ductility. However, relative to the initial state (after quenching), the offset yield strength increased on average by ~2.5 times, the ultimate tensile stress limit by ~1.7 times, and the elongation increased by 10. The properties after annealing for 30 and 120 min were approximately equal.

The structure of L68 brass after rotary swaging and additional annealing consists predominantly of fine equiaxed grains (Fig. 5). After annealing for 30 min, the average size is 3.1±0.4 μm; with an increase in the heating duration to 120 min, the grains increase slightly to 4.5±0.8 μm. It should also be noted that individual twins no more than 1 μm wide are formed inside the recrystallized grains (Fig. 6).

DISCUSSION

The study of the influence of cold rotary swaging and subsequent annealing on the structure and mechanical properties of L68 brass showed that rotary swaging leads to the formation of a microstructure in the alloy, which is elongated along the direction of deformation (Fig. 1), as well as to the formation of a UFG microstructure inside the elongated grains and a significant increase in the density of crystal lattice defects (Fig. 2). Such a change in the microstructure leads to a significant increase in the strength of the alloy (yield strength and ultimate tensile stress limit increase by ~10 and ~3.5 times, respectively), but greatly reduces its ductility (δ decreases from 39.9±3.8 to 6.3±0.4 %).

The conducted DSC analysis showed that all the identified transformations occur with energy absorption (Fig. 3). Thus, the first peaks on swaged brass (~213 and ~301 °C) probably correspond to the ongoing processes of polygonisation and recovery. Similar results were obtained during the DSC analysis of cold-formed wire made of LS59-1 lead brass, where the authors revealed the occurrence of these processes in the temperature range of 115–235 °C [22]. The next peak on the curve for the swaged alloy, corresponding to ~433 °C, is probably associated with the onset of recrystallization processes. It is known that in deformed pure copper, the recrystallization process begins to occur at 250–350 °C [23; 24]. The recrystallisation onset temperature

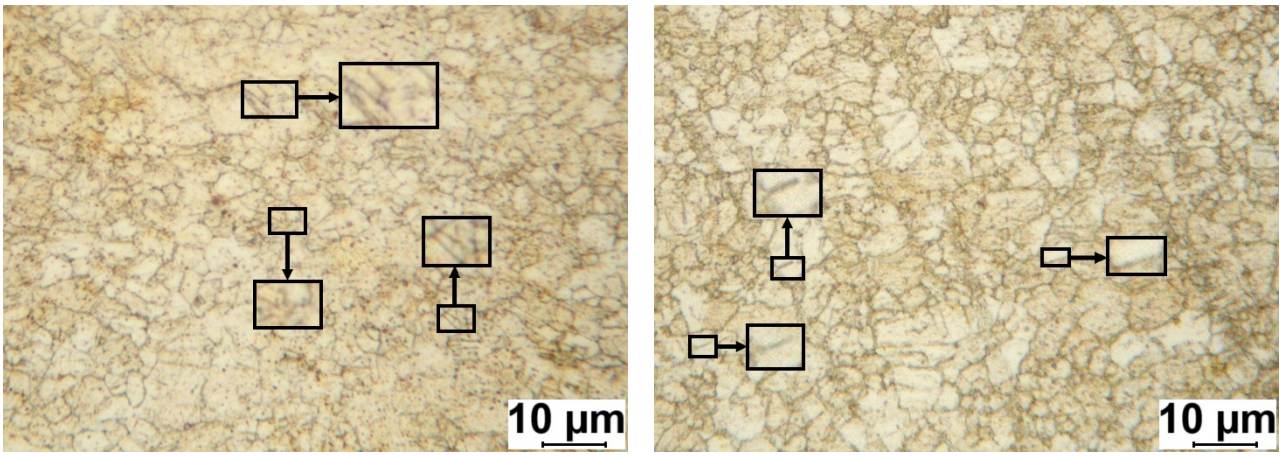

a ***b***

Fig. 6. *Microstructure of L68 brass after rotary swaging at room temperature and subsequent annealing for 30 min (**a**) and 2 h (**b**). Arrows indicate twins*
Рис. 6. *Микроструктура латуни Л68 после ротационной ковки при комнатной температуре и последующего отжига в течение 30 мин (**а**) и 2 ч (**b**). Стрелки указывают на двойники*

in this case depends on the purity of copper, the degree of deformation and the heating rate of the samples during the study. The addition of alloying elements increases the recrystallization temperature, in this case to ~433 °C. The fact that recrystallization occurs at this temperature is also confirmed by microstructural studies (Fig. 6). Thus, annealing of the alloy at 450 °C causes the formation of small equiaxed grains with individual twins. In this case, increasing the annealing time from 30 min to 2 h has little effect on the size of the forming grain, causing only a slight increase from 3.1±0.4 to 4.5±0.8 μm. In this case, the peaks corresponding to ~560 and ~626 °C are apparently associated either with the further course of primary recrystallisation, or with the onset of collective and secondary recrystallization.

The formation of a recrystallised structure after annealing caused a significant decrease in the strength of L68 brass relative to the swaged state (Fig. 5, Table 1). Thus, the modulus of rapture in this case decreased by ~4.2 times and the ultimate tensile stress limit – by ~2 times. However, it is worth noting that the obtained values of the strength characteristics significantly exceed the values obtained for the quenched alloy: by ~2.5 and ~1.7 times for $\sigma_{0.2}$ and σ_B, respectively. In this case, the relative elongation values increase both in comparison with the swaged state (by ~7.9 times) and with respect to the quenched state (by ~10 %). It is worthy of note that the mechanical properties of L68 brass annealed for 30 min and 2 h are practically the same. The increase in the alloy strength after rotary swaging is largely related to the refinement of the alloy microstructure and an increase in the dislocation density.

As is known, the increase in the strength of metals and alloys is mainly influenced by such factors as grain size, the presence of second-phase particles, an increase in the density of crystal lattice defects, in particular dislocations, and the formation of a solid solution [25]. In the study, the presence of second-phase particles was not detected in any of the alloy states, so the contribution of this mechanism can be neglected. On the other hand, the alloy contains 32±0.13 wt. % of Zn, which is completely dissolved in the copper matrix, forming a solid solution. The presence of zinc increases the strength characteristics of pure copper. However, as was said above, the alloy structure in all three states (quenched, swaged and annealed) consists of grains of a solid solution of zinc in copper of different sizes. This means that the contribution of the solid-solution mechanism to strengthening has a similar value for different states of the alloy. At the same time, rotary swaging leads to a significant grain refinement relative to the quenched state. Moreover, rotary swaging, like any deformation treatment, causes an increase in the dislocation density. For example, in [26] it was shown that during rotary swaging of the Cu–3.11Cr copper alloy, an increase in the dislocation density was observed from 3.87×10^{11} m^{-2} in the quenched state to 1.22×10^{15} m^{-2} after rotary swaging. Therefore, a significant increase in the dislocation density should also be expected in this experiment. Subsequent annealing at 450 °C leads both to an increase in the grain size to 3–5 μm due to the recrystallization and to a decrease in the dislocation density. In [26], the dislocation density of the Cu–3.11Cr alloy after rotary swaging with subsequent aging in the temperature range from 400 to 550 °C was also calculated. It was shown that heating in this temperature range leads to a slight decrease in the dislocation density to 9.41×10^{14} m^{-2}. Grain growth and a decrease in dislocation density lead to a decrease in the contribution of these mechanisms to strengthening, which results in a decrease in the strength characteristics. At the same time, the formation of small, recrystallized grains and a decrease in dislocation density lead to a significant improvement in the ductility of the alloy. A similar picture was observed in [27] during annealing at various temperatures of the Cu–4.5 wt. % Al alloy subjected to rotary swaging. The authors showed that an increase in the temperature and duration of annealing leads to grain growth due to recrystallization, which has a positive effect on ductility.

Summarizing the obtained data, one can conclude that rotary swaging significantly increases the strength characteristics of L68 brass with a decrease in its ductility, while subsequent annealing allows obtaining a state with improved strength and ductility values relative to the quenched state. At the same time, both swaged and annealed alloys can be successfully used in the national economy to solve various tasks, since the mechanical characteristics obtained in the work are not inferior to the values regulated by GOST 494-90, GOST 1066-2015, GOST 931-90 and GOST 5362-78 or even exceed them (Table 2). For example, brass after rotary swaging can be used in

Table 2. *Comparison of the requirements for processed L68 brass with the data obtained in the work*
Таблица 2. *Сравнение требований, предъявляемых к обработанной латуни Л68, с полученными в работе данными*

Application / processing technique	σ_B, MPa	δ, %	Source
Soft wire (diameter 0.18–0.75 mm)	340	25	GOST 1066-2015
Hard-drawn wire (diameter 0.18–0.75 mm)	690–930	–	GOST 1066-2015
Cold-rolled hard band	430–540	10	GOST 931-90
Cold-rolled band	290–370	42	GOST 931-90
Cold-rolled band	290–340	50	GOST 5362-78

Table 2 continued
Продолжение таблицы 2

Application / processing technique	σ_B, MPa	δ, %	Source
Soft pipe	290	40	GOST 494-90
Half-hard pipe	340	35	GOST 494-90
Rotary swaging (ε=2.31)	775±6	6.3±0.4	Current study
Rotary swaging (ε=2.31) + heating 450 °C (30 min)	382±4	49.1±1.4	Current study

the manufacture of products that require high strength indicators, for example, those operating under abrasion conditions. L68 brass annealed after rotary swaging can be used in the manufacture of products for which a combination of strength and ductility is important, for example, plumbing products. Moreover, rotary swaging processing can be easily combined with other deformation methods, for example, with drawing. It is assumed that such a combination can lead to an additional improvement in mechanical characteristics.

CONCLUSIONS

1. Rotary swaging of L68 brass leads to the formation of α-phase grains elongated along the deformation direction, within which a UFG structure is formed consisting of subgrains 300–400 nm in size, deformation twins from several tens to 200 nm in width, and shear bands 400–500 nm in width.

2. After annealing at 450 °C, a recrystallised microstructure with a grain size of 3.1±0.4 and 4.5±0.8 μm is formed for 30 min and 2 h of holding, respectively.

3. The formation of a UFG structure after rotary swaging leads to an increase in $\sigma_{0.2}$ and σ_B by ~10 and ~3.5 times, respectively, with a decrease in ductility from 39.9±3.8 to 6.3±0.4 %. Subsequent annealing at 450 °C resulted in a decrease in the strength characteristics of L68 brass due to recrystallization with a simultaneous increase in the relative elongation value to ~49 %.

4. The duration of annealing at 450 °C did not affect the value of the mechanical characteristics of the alloy.

REFERENCES

1. Yang Kuo, Wang Yihan, Guo Mingxing, Wang Hu, Mo Yongda, Dong Xueguang, Lou Huafen. Recent development of advanced precipitation-strengthened Cu alloys with high strength and conductivity: a review. *Progress in Materials Science*, 2023, vol. 138, article number 101141. DOI: 10.1016/j.pmatsci.2023.101141.
2. Mousavi S.E., Sonboli A., Naghshehkesh N., Meratian M., Salehi A., Sanayei M. Different behavior of alpha and beta phases in a Low Stacking Fault Energy copper alloy under severe plastic deformation. *Materials Science and Engineering: A*, 2020, vol. 788, article number 139550. DOI: 10.1016/j.msea.2020.139550.
3. Imai H., Li S., Atsumi H., Kosaka Y., Kojima A., Umeda J., Kondoh K. Mechanical Properties and Machinability of Extruded Cu-40% Zn Brass Alloy with Bismuth via Powder Metallurgy Process. *Transactions of JWRI*, 2009, vol. 38, no. 1, pp. 25–30. DOI: 10.18910/5502.
4. Basori I., Gadhu R., Sofyan B.T. Effects of deformation and annealing temperature on the microstructures and mechanical properties of Cu-32% Zn Brass. *ARPN Journal of Engineering and Applied Sciences*, 2016, vol. 11, no. 4, pp. 2741–2745. DOI: 10.4028/www.scientific.net/KEM.748.218.
5. Galai M., Ouassir J., Ebn Touhami M., Nassali H., Benqlilou H., Belhaj T., Berrami K., Mansouri I., Oauki B. α-Brass and (α+β) Brass Degradation Processes in Azrou Soil Medium Used in Plumbing Devices. *Journal of Bio-and Tribo-Corrosion*, 2017, vol. 3, no. 3, article number 30. DOI: 10.1007/s40735-017-0087-y.
6. Pelto-Huikko A., Salonen N., Latva M. Dezincification of faucets with different brass alloys. *Engineering Failure Analysis*, 2025, vol. 169, article number 109202. DOI: 10.1016/j.engfailanal.2024.109202.
7. Valiev R.Z., Islamgaliev R.K., Alexandrov I.V. Bulk nanostructured materials from severe plastic deformation. *Progress in materials science*, 2000, vol. 45, no. 2, pp. 103–189. DOI: 10.1016/S0079-6425(99)00007-9.
8. Vidilli A.L., Machado I.F., Edalati K., Botta W.J., Bolfarini C., Koga G.Y. Wear-resistant ultrafine severely deformed brass (Cu-30Zn). *Materials Letters*, 2024, vol. 377, article number 137465. DOI: 10.1016/j.matlet.2024.137465.
9. Chen Jianqing, Su Yehan, Zhang Qiyu, Sun Jiapeng, Yang Donghui, Jiang Jinghua, Song Dan, Ma Aibin. Enhancement of strength-ductility synergy in ultrafine-grained Cu-Zn alloy prepared by ECAP and subsequent annealing. *Journal of Materials Research and Technology*, 2022, vol. 17, pp. 433–440. DOI: 10.1016/j.jmrt.2022.01.026.
10. Shahriyari F., Shaeri M.H., Dashti A., Zarei Z., Noghani M.T., Cho Jae Hyung, Djavanroodi F. Evolution of mechanical properties, microstructure and texture and of various brass alloys processed by multi-directional forging. *Materials Science and Engineering: A*, 2022, vol. 831, article number 142149. DOI: 10.1016/j.msea.2021.142149.
11. Radhi H.N., Mohammed M.T. Aljassani A.M.H. Influence of ECAP processing on mechanical and wear properties of brass alloy. *Materials Today: Proceedings*, 2021, vol. 44, pp. 2399–2402. DOI: 10.1016/j.matpr.2020.12.461.
12. Konkova T., Mironov S., Korznikov A., Korznikova G., Myshlyaev M., Semiatin L. A two-step approach for producing an ultrafine-grain structure in Cu–30Zn brass.

Materials Letters. *Materials Letters*, 2015, vol. 161, pp. 1–4. DOI: 10.1016/j.matlet.2015.08.025.
13. Mao Qingzhong, Liu Yanfang, Zhao Yonghao. A review on mechanical properties and microstructure of ultrafine grained metals and alloys processed by rotary swaging. *Journal of Alloys and Compounds*, 2022, vol. 896, article number 163122. DOI: 10.1016/j.jallcom.2021.163122.
14. Naydenkin E.V., Mishin I.P., Zabudchenko O.V., Lykova O.N., Manisheva A.I. Structural-phase state and mechanical properties of β titanium alloy produced by rotary swaging with subsequent aging. *Journal of Alloys and Compounds*, 2023, vol. 935, article number 167973. DOI: 10.1016/j.jallcom.2022.167973.
15. Chuvil’deev V.N., Kopylov V.I., Nokhrin A.V. et al. Enhancement of the Strength and the Corrosion Resistance of a PT-7M Titanium Alloy Using Rotary Forging. *Russian Metallurgy (Metally)*, 2021, vol. 2021, no. 5, pp. 600–610. DOI: 10.1134/S0036029521050050.
16. Mao Qingzhong, Wang Long, Nie Jinfeng, Zhao Yonghao. Optimizing strength and electrical conductivity of 6201 aluminum alloy wire through rotary swaging and aging processes. *Journal of Materials Processing Technology*, 2024, vol. 331, article number 118497. DOI: 10.1016/j.jmatprotec.2024.118497.
17. Dedyulina O.K., Salishchev G.A. Formation of ultrafine-grained structure in medium-carbon steel 40HGNM by swaging and its influence on mechanical properties. *Fundamental research*, 2013, no. 1-3, pp. 701–706. EDN: PUUIVF.
18. Martynenko N.S., Bochvar N.R., Rybalchenko O.V., Prosvirnin D.V., Rybalchenko G.V., Kolmakov A.G., Morozov M.M., Yusupov V.S., Dobatkin S.V. Increase in the strength and electrical conductivity of a Cu–0.8 Hf alloy after rotary swaging and subsequent aging. *Russian Metallurgy (Metally)*, 2023, vol. 2023, no. 4, pp. 466–474. DOI: 10.1134/S0036029523040158.
19. Martynenko N., Rybalchenko O., Straumal P. et al. Increasing strength and electrical conductivity of Cu-0.77% Cr-0.86% Hf alloy by rotary swaging and subsequent aging. *Journal of Materials Science*, 2024, vol. 59, pp. 5944–5955. DOI: 10.1007/s10853-024-09332-x.
20. Martynenko N., Rybalchenko O., Bodyakova A., Prosvirnin D., Rybalchenko G., Morozov M., Yusupov V., Dobatkin S. Effect of Rotary Swaging on the Structure, Mechanical Characteristics and Aging Behavior of Cu-0.5%Cr-0.08%Zr Alloy. *Materials*, 2023, vol. 16, no. 1, article number 105. DOI: 10.3390/ma16010105.
21. Martynenko N.S., Bochvar N.R., Rybalchenko O.V., Bodyakova A.I., Morozov M.M., Leonova N.P., Yusupov V.S., Dobatkin S.V. Effect of rotary swaging and subsequent aging on the structure and mechanical properties of a Cu-0.5% Cr-0.08% Zr alloy. *Russian metallurgy* (*Metally)*, 2022, vol. 2022, no. 5, pp. 512–519. DOI: 10.1134/S0036029522050081.
22. Illarionov A.G., Loginov Y.N., Stepanov S.I., Illarionova S.M., Radaev P.S. Variation of the Structure-and-Phase Condition and Physical and Mechanical Properties of Cold-Deformed Leaded Brass Under Heating. *Metal Science and Heat Treatment*, 2019, vol. 61, pp. 243–248. DOI: 10.1007/s11041-019-00408-z.
23. Chen Jian, Ma Xiao-guang, Li Jun, Yao Yu-hong, Yan Wen, Fan Xin-hui. New method for analyzing recrystallization kinetics of deformed metal by differential scanning calorimeter. *Journal of Central South University*, 2015, vol. 22, pp. 849–854. DOI: 10.1007/s11771-015-2592-9.
24. Benchabane G., Boumerzoug Z., Thibon I., Gloriant T. Recrystallization of pure copper investigated by calorimetry and microhardness. *Materials Characterization*, 2008, vol. 59, no. 10, pp. 1425–1428. DOI: 10.1016/j.matchar.2008.01.002.
25. Sitdikov V.D., Khafizova E.D., Polenok M.V. Microstructure and properties of the Zn-1%Li-2%Mg alloy subjected to severe plastic deformation. *Frontier Materials & Technologies*, 2023, no. 2, pp. 117–130. DOI: 10.18323/2782-4039-2023-2-64-7.
26. Mao Qingzhong, Wang Long, Nie Jinfeng, Zhao Yonghao. Enhancing strength and electrical conductivity of Cu–Cr composite wire by two-stage rotary swaging and aging treatments. *Composites Part B: Engineering*, 2022, vol. 231, article number 109567. DOI: 10.1016/j.compositesb.2021.109567.
27. Li Xingfu, Li Cong, Sun Lele, Gong Yulan, Pan Hongjiang, Tan Zhilong, Xu Lei, Zhu Xinkun. Enhancing strength-ductility synergy of Cu alloys with heterogeneous microstructure via rotary swaging and annealing. *Materials Science and Engineering: A*, 2025, vol. 920, article number 147501. DOI: 10.1016/j.msea.2024.147501.

СПИСОК ЛИТЕРАТУРЫ

1. Yang Kuo, Wang Yihan, Guo Mingxing, Wang Hu, Mo Yongda, Dong Xueguang, Lou Huafen. Recent development of advanced precipitation-strengthened Cu alloys with high strength and conductivity: a review // Progress in Materials Science. 2023. Vol. 138. Article number 101141. DOI: 10.1016/j.pmatsci.2023.101141.
2. Mousavi S.E., Sonboli A., Naghshehkesh N., Meratian M., Salehi A., Sanayei M. Different behavior of alpha and beta phases in a Low Stacking Fault Energy copper alloy under severe plastic deformation // Materials Science and Engineering: A. 2020. Vol. 788. Article number 139550. DOI: 10.1016/j.msea.2020.139550.
3. Imai H., Li S., Atsumi H., Kosaka Y., Kojima A., Umeda J., Kondoh K. Mechanical Properties and Machinability of Extruded Cu-40% Zn Brass Alloy with Bismuth via Powder Metallurgy Process // Transactions of JWRI. 2009. Vol. 38. № 1. P. 25–30. DOI: 10.18910/5502.
4. Basori I., Gadhu R., Sofyan B.T. Effects of deformation and annealing temperature on the microstructures and mechanical properties of Cu-32% Zn Brass // ARPN Journal of Engineering and Applied Sciences. 2016. Vol. 11. № 4. P. 2741–2745. DOI: 10.4028/www.scientific.net/KEM.748.218.
5. Galai M., Ouassir J., Ebn Touhami M., Nassali H., Benqlilou H., Belhaj T., Berrami K., Mansouri I., Oauki B. α-Brass and (α+β) Brass Degradation Processes in Azrou Soil Medium Used in Plumbing Devices // Journal of Bio-and Tribo-Corrosion. 2017. Vol. 3. № 3. Article number 30. DOI: 10.1007/s40735-017-0087-y.
6. Pelto-Huikko A., Salonen N., Latva M. Dezincification of faucets with different brass alloys // Engineering Failure Analysis. 2025. Vol. 169. Article number 109202. DOI: 10.1016/j.engfailanal.2024.109202.

7. Valiev R.Z., Islamgaliev R.K., Alexandrov I.V. Bulk nanostructured materials from severe plastic deformation // Progress in materials science. 2000. Vol. 45. № 2. P. 103–189. DOI: 10.1016/S0079-6425(99)00007-9.
8. Vidilli A.L., Machado I.F., Edalati K., Botta W.J., Bolfarini C., Koga G.Y. Wear-resistant ultrafine severely deformed brass (Cu-30Zn) // Materials Letters. 2024. Vol. 377. Article number 137465. DOI: 10.1016/j.matlet.2024.137465.
9. Chen Jianqing, Su Yehan, Zhang Qiyu, Sun Jiapeng, Yang Donghui, Jiang Jinghua, Song Dan, Ma Aibin. Enhancement of strength-ductility synergy in ultrafine-grained Cu-Zn alloy prepared by ECAP and subsequent annealing // Journal of Materials Research and Technology. 2022. Vol. 17. P. 433–440. DOI: 10.1016/j.jmrt.2022.01.026.
10. Shahriyari F., Shaeri M.H., Dashti A., Zarei Z., Noghani M.T., Cho Jae Hyung, Djavanroodi F. Evolution of mechanical properties, microstructure and texture and of various brass alloys processed by multi-directional forging // Materials Science and Engineering: A. 2022. Vol. 831. Article number 142149. DOI: 10.1016/j.msea.2021.142149.
11. Radhi H.N., Mohammed M.T. Aljassani A.M.H. Influence of ECAP processing on mechanical and wear properties of brass alloy // Materials Today: Proceedings. 2021. Vol. 44. P. 2399–2402. DOI: 10.1016/j.matpr.2020.12.461.
12. Konkova T., Mironov S., Korznikov A., Korznikova G., Myshlyaev M., Semiatin L. A two-step approach for producing an ultrafine-grain structure in Cu–30Zn brass. Materials Letters // Materials Letters. 2015. Vol. 161. P. 1–4. DOI: 10.1016/j.matlet.2015.08.025.
13. Mao Qingzhong, Liu Yanfang, Zhao Yonghao. A review on mechanical properties and microstructure of ultrafine grained metals and alloys processed by rotary swaging // Journal of Alloys and Compounds. 2022. Vol. 896. Article number 163122. DOI: 10.1016/j.jallcom.2021.163122.
14. Naydenkin E.V., Mishin I.P., Zabudchenko O.V., Lykova O.N., Manisheva A.I. Structural-phase state and mechanical properties of β titanium alloy produced by rotary swaging with subsequent aging // Journal of Alloys and Compounds. 2023. Vol. 935. Article number 167973. DOI: 10.1016/j.jallcom.2022.167973.
15. Chuvil’deev V.N., Kopylov V.I., Nokhrin A.V. et al. Enhancement of the Strength and the Corrosion Resistance of a PT-7M Titanium Alloy Using Rotary Forging // Russian Metallurgy (Metally). 2021. Vol. 2021. № 5. P. 600–610. DOI: 10.1134/S0036029521050050.
16. Mao Qingzhong, Wang Long, Nie Jinfeng, Zhao Yonghao. Optimizing strength and electrical conductivity of 6201 aluminum alloy wire through rotary swaging and aging processes // Journal of Materials Processing Technology. 2024. Vol. 331. Article number 118497. DOI: 10.1016/j.jmatprotec.2024.118497.
17. Дедюлина О.К., Салищев Г.А. Формирование ультрамелкозернистой структуры в среднеуглеродистой стали 40ХГНМ ротационной ковкой и ее влияние на механические свойства // Фундаментальные исследования. 2013. № 1-3. С. 701–706. EDN: PUUIVF.
18. Martynenko N.S., Bochvar N.R., Rybalchenko O.V., Prosvirnin D.V., Rybalchenko G.V., Kolmakov A.G., Morozov M.M., Yusupov V.S., Dobatkin S.V. Increase in the strength and electrical conductivity of a Cu–0.8 Hf alloy after rotary swaging and subsequent aging // Russian Metallurgy (Metally). 2023. Vol. 2023. № 4. P. 466–474. DOI: 10.1134/S0036029523040158.
19. Martynenko N., Rybalchenko O., Straumal P. et al. Increasing strength and electrical conductivity of Cu-0.77% Cr-0.86% Hf alloy by rotary swaging and subsequent aging // Journal of Materials Science. 2024. Vol. 59. P. 5944–5955. DOI: 10.1007/s10853-024-09332-x.
20. Martynenko N., Rybalchenko O., Bodyakova A., Prosvirnin D., Rybalchenko G., Morozov M., Yusupov V., Dobatkin S. Effect of Rotary Swaging on the Structure, Mechanical Characteristics and Aging Behavior of Cu-0.5%Cr-0.08%Zr Alloy // Materials. 2023. Vol. 16. № 1. Article number 105. DOI: 10.3390/ma16010105.
21. Мартыненко Н.С., Бочвар Н.Р., Рыбальченко О.В., Бодякова А.И., Морозов М.М., Леонова Н.П., Юсупов В.С., Добаткин С.В. Влияние ротационной ковки и последующего старения на структуру и механические свойства сплава Cu-0,5%Cr-0,08%Zr // Металлы. 2022. № 3. С. 56–64. EDN: MQEZDH.
22. Illarionov A.G., Loginov Y.N., Stepanov S.I., Illarionova S.M., Radaev P.S. Variation of the Structure-and-Phase Condition and Physical and Mechanical Properties of Cold-Deformed Leaded Brass Under Heating // Metal Science and Heat Treatment. 2019. Vol. 61. P. 243–248. DOI: 10.1007/s11041-019-00408-z.
23. Chen Jian, Ma Xiao-guang, Li Jun, Yao Yu-hong, Yan Wen, Fan Xin-hui. New method for analyzing recrystallization kinetics of deformed metal by differential scanning calorimeter // Journal of Central South University. 2015. Vol. 22. P. 849–854. DOI: 10.1007/s11771-015-2592-9.
24. Benchabane G., Boumerzoug Z., Thibon I., Gloriant T. Recrystallization of pure copper investigated by calorimetry and microhardness // Materials Characterization. 2008. Vol. 59. № 10. P. 1425–1428. DOI: 10.1016/j.matchar.2008.01.002.
25. Ситдиков В.Д., Хафизова Э.Д., Поленок М.В. Микроструктура и свойства сплава Zn–1%Li–2%Mg, подвергнутого интенсивной пластической деформации // Frontier Materials & Technologies. 2023. № 2. С. 117–130. DOI: 10.18323/2782-4039-2023-2-64-7.
26. Mao Qingzhong, Wang Long, Nie Jinfeng, Zhao Yonghao. Enhancing strength and electrical conductivity of Cu–Cr composite wire by two-stage rotary swaging and aging treatments // Composites Part B: Engineering. 2022. Vol. 231. Article number 109567. DOI: 10.1016/j.compositesb.2021.109567.
27. Li Xingfu, Li Cong, Sun Lele, Gong Yulan, Pan Hongjiang, Tan Zhilong, Xu Lei, Zhu Xinkun. Enhancing strength-ductility synergy of Cu alloys with heterogeneous microstructure via rotary swaging and annealing // Materials Science and Engineering: A. 2025. Vol. 920. Article number 147501. DOI: 10.1016/j.msea.2024.147501.

УДК 669.2:669.35:621.73.043:539.424
doi: 10.18323/2782-4039-2025-3-73-9

Влияние ротационной ковки и последующего отжига на структуру и механические свойства однофазной латуни Л68

Чистюхина Элеонора Ивановна*[1,2,4], инженер-исследователь лаборатории металловедения цветных и легких металлов им. академика А.А. Бочвара, магистрант кафедры металловедения и физики прочности
Мартыненко Наталья Сергеевна[1,5], кандидат технических наук, старший научный сотрудник лаборатории металловедения цветных и легких металлов им. академика А.А. Бочвара
Рыбальченко Ольга Владиславовна[1,6], кандидат технических наук, ведущий научный сотрудник лаборатории металловедения цветных и легких металлов им. академика А.А. Бочвара
Никитин Иван Сергеевич[3,7], кандидат технических наук, младший научный сотрудник лаборатории механических свойств наноструктурных и жаропрочных материалов
Лукьянова Елена Александровна[1,8], кандидат технических наук, старший научный сотрудник лаборатории металловедения цветных и легких металлов им. академика А.А. Бочвара
Горбенко Артем Дмитриевич[1,9], инженер-исследователь лаборатории прочности и пластичности металлических и композиционных материалов и наноматериалов
Темралиева Диана Ривовна[1,10], инженер-исследователь лаборатории металловедения цветных и легких металлов им. академика А.А. Бочвара
Страумал Петр Борисович[1,11], кандидат физико-математических наук, старший научный сотрудник лаборатории металловедения цветных и легких металлов им. академика А.А. Бочвара
Андреев Владимир Александрович[1,12], кандидат технических наук, ведущий научный сотрудник лаборатории пластической деформации металлических материалов
Добаткин Сергей Владимирович[1,13], доктор технических наук, профессор, заведующий лабораторией металловедения цветных и легких металлов им. академика А.А. Бочвара
[1]*Институт металлургии и материаловедения им. А.А. Байкова РАН, Москва (Россия)*
[2]*Университет науки и технологий МИСИС, Москва (Россия)*
[3]*Белгородский государственный национальный исследовательский университет, Белгород (Россия)*

***E-mail:** e.chistyuhina@mail.ru

[4]ORCID: https://orcid.org/0009-0009-2192-3246
[5]ORCID: https://orcid.org/0000-0003-1662-1904
[6]ORCID: https://orcid.org/0000-0002-0403-0800
[7]ORCID: https://orcid.org/0000-0002-5417-9857
[8]ORCID: https://orcid.org/0000-0001-7122-6427
[9]ORCID: https://orcid.org/0000-0002-3357-4049
[10]ORCID: https://orcid.org/0000-0002-8392-7826
[11]ORCID: https://orcid.org/0000-0001-6192-5304
[12]ORCID: https://orcid.org/0000-0003-3937-1952
[13]ORCID: https://orcid.org/0000-0003-4232-927X

Поступила в редакцию 30.06.2025 *Пересмотрена 18.07.2025* *Принята к публикации 25.08.2025*

Аннотация: Медные сплавы на основе системы Cu–Zn, в частности латунь Л68, являются перспективными конструкционными материалами. Однако для повышения их надежности и расширения области применения необходимо повышать их прочностные характеристики. В работе изучалось влияние комбинации ротационной ковки (РК) и последующего отжига на структуру, прочность и пластичность латуни Л68. Для этого проведены исследования микроструктуры сплава в закаленном и деформированном состояниях, механические испытания на одноосное растяжение, исследование твердости по методу Бринелля, а также оценка структурно-фазовых переходов методом дифференциальной сканирующей калориметрии. Установлено, что в процессе РК происходит формирование не только вытянутых вдоль направления деформации зерен α-фазы, но и ультрамелкозернистой структуры внутри них, состоящей из субзерен, двойников деформации и полос сдвига. Последующий отжиг при 450 °С приводит к росту размера зерна до 3–5 мкм за счет протекания статической рекристаллизации. После РК наблюдается рост условного предела текучести ($\sigma_{0,2}$) и предела прочности (σ_B) в ~10 и ~3,5 раза соответственно при снижении значения относительного удлинения более чем в 6 раз. Последующий отжиг при 450 °С, вызвавший формирование рекристаллизованной структуры, привел к снижению прочностных характеристик латуни Л68 относительно деформированного состояния при одновременном росте значения относительного удлинения по сравнению как с деформированным, так и с исходным состоянием сплава. Однако стоит отметить, что $\sigma_{0,2}$ и σ_B латуни Л68 после РК и последующего отжига при 450 °С превышают значения для зака-

ленного сплава в среднем в ~2,5 и в ~1,7 раза соответственно и превышают значения, регламентированные ГОСТ 494-90, ГОСТ 1066-2015, ГОСТ 931-90 и ГОСТ 5362-78.

Ключевые слова: латунь Л68; ротационная ковка; ультрамелкозернистая структура; рекристаллизация; прочность; пластичность.

Благодарности: Работа выполнена при финансовой поддержке государственного задания № 075-00319-25-00.

Статья подготовлена по материалам докладов участников XII Международной школы «Физическое материаловедение» (ШФМ-2025), Тольятти, 15–19 сентября 2025 года.

Для цитирования: Чистюхина Э.И., Мартыненко Н.С., Рыбальченко О.В., Никитин И.С., Лукьянова Е.А., Горбенко А.Д., Темралиева Д.Р., Страумал П.Б., Андреев В.А., Добаткин С.В. Влияние ротационной ковки и последующего отжига на структуру и механические свойства однофазной латуни Л68 // Frontier Materials & Technologies. 2025. № 3. С. 113–124. DOI: 10.18323/2782-4039-2025-3-73-9.